

PCCP

Accepted Manuscript



This is an *Accepted Manuscript*, which has been through the Royal Society of Chemistry peer review process and has been accepted for publication.

Accepted Manuscripts are published online shortly after acceptance, before technical editing, formatting and proof reading. Using this free service, authors can make their results available to the community, in citable form, before we publish the edited article. We will replace this *Accepted Manuscript* with the edited and formatted *Advance Article* as soon as it is available.

You can find more information about *Accepted Manuscripts* in the [Information for Authors](#).

Please note that technical editing may introduce minor changes to the text and/or graphics, which may alter content. The journal's standard [Terms & Conditions](#) and the [Ethical guidelines](#) still apply. In no event shall the Royal Society of Chemistry be held responsible for any errors or omissions in this *Accepted Manuscript* or any consequences arising from the use of any information it contains.

Detonation nanodiamond coating effect on thermal decomposition properties of RDX explosive

Yi Tong,* Rui Liu and Tonglai Zhang

Abstract

The well-dispersed and uniformly shaped detonation nanodiamond (DND) was produced and coated over micron RDX in various amounts to form four kinds of DND coating composites (NDRs). In order to confirm the optimal coating amount and its effect on the thermal properties, the thermal decomposition and kinetics were studied by DSC, TG and DPTA techniques. The critical temperature of thermal explosion (T_b) and self accelerating decomposition temperature (T_{SADT}) both exhibit an interesting volcano-shaped changing trend and rank in increasing order of $NDR4 < NDR1 < RDX < NDR3 < NDR2$. It indicates that the DND coating amount ranging from 1/7 to 1/5 provides NDR with better thermal safety than RDX. The thermolytic kinetic parameters (E_a and A) and activation thermodynamic parameters (ΔS^\ddagger , ΔH^\ddagger and ΔG^\ddagger) are sorted in order of $NDR1 < NDR4 < NDR2 < NDR3$. The gas emission and reaction rate constant of the initial thermal decomposition have the same order. The results show that the DND coating could improve the reactivity of NDRs and such effect is proportional to its coating amount. However, excessive coating that is more than 1/3, like a layer of protective shell, conversely hinders the decomposition and gas diffusion. The isoconversional activation energies (E_a) vary with conversion extent (α) at the initial stage of $\alpha = 0.1\sim 0.5$, which indicates that the thermal decomposition of NDR is a multi-step process including the secondary reaction or catalytic reaction. However, the E_a s are almost independent on α when $\alpha = 0.6\sim 0.9$ with the mean values in increasing order of $NDR1 < NDR4 < NDR2 < NDR3$.

* School of Mechatronic Engineering, Beijing Institute of Technology. No.5, Zhongguancun South Street, Beijing, 100081(China). Tel & Fax: (+8610) 68911134, E-mail: tongyi@bit.edu.cn (corresponding author: Yi Tong)

Introduction

Diamond is an outstanding material in many respects, and nanodiamond inherits most of the superior properties of bulk diamond and delivers them at the nanoscale.¹ Nanodiamond (ND) exhibits excellent mechanical and optical properties, high hardness, huge surface area, high thermal conductivity and electrical resistivity. More importantly, it is also non-toxic, environmentally benign and chemically reactive.²⁻⁴ The advantages open an important application in fabricating the novel ND-based composites with more outstanding properties by coating and doping techniques.⁵⁻¹⁶

Hexahydro-1,3,5-trinitro-1,3,5-triazine (RDX) is a widely used high energy explosive. It has occupied a key position in the main charge explosive of warheads and the energetic component of composite propellants.¹⁷⁻¹⁹ The improvement of thermolytic and detonation properties of RDX is a hot topic recently. Current international investigations on hybrid systems try to find out the best formulation of solid explosives in order to increase the energy output on the one hand; on the other hand the effort is to keep the intrinsic safety of such high-energy materials, as well as low environmental impact and overall cost.^{20, 21} The common way of modification consists in adding energetic additives into its formulation. Research on the use of such additives, in particular nano metal powders including Al, Cu and Ni, have been conducted for several years in order to investigate the effects on the thermal and mechanical properties of composite explosives.²²⁻²⁶ The use of nano metal powders appears to be quite promising due to the high enthalpy release, high surface reactivity and density increase. However, such powders without any coating layers tend to oxidize significantly (at worst to self-ignite) immediately after production as a result of contact with an oxidizing medium. Moreover, the nano metal powders have the disadvantages of heavy metal pollution and poor cost efficiency. Considering that ND is a good choice of additive for composites, RDX coated by ND is certain to exhibit some exceptional performances. However, little research has been carried out due to the potential hazards in modification of explosives and the difficulties in preparation of well-dispersed ND. Thus, in this work, four kinds of ND coating RDX composites with various coating amounts were prepared, and the thermal decomposition and kinetics were studied by DSC, TG and DPTA techniques.

Experimental

Preparation of detonation nanodiamond (DND)

ND was prepared by the detonation of the explosive mixture of 60 wt% TNT and 40 wt% RDX in a closed metallic chamber owing to the lack of oxygen and the resulting incomplete oxidation.²⁷⁻²⁹ Thereinto, TNT produced most of the soot and RDX contributed the major part of the energy. During detonation, the pressure and temperature raised dramatically (the temperature of 3000~4000 K and the pressure of 20~30 GPa), instantaneously forming the thermodynamically stable ND particles. Such resulting ND is generally referred to as detonation nanodiamond (DND). After detonation, the diamond-containing soot was collected from the bottom and the walls of the chamber. However, the crude products were covered by the carbon allotropes (such as graphitic materials) and impurities (generally iron and other metals from the steel walls of the detonation chamber) as the soot formation continued even after the pressure dropped. Therefore, a thorough purification was needed to obtain the refined DND. The metal impurities were removed by acidification using hydrochloric acid under heating. The non-diamond carbon materials were removed via oxidation using concentrated nitric acid and fuming sulfuric acid, both of which were preheated to boiling. The purified DND tends to agglomerate to larger particles due to their large specific surface area. Therefore, a surfactant (dispersant) should be used to protect DND against agglomeration and keep them well dispersed both in solid and liquid. Sorbitan monooleate ($C_{24}H_{44}O_6$), Span-80, was selected as a surfactant according to empirical experiment.

Preparation of DND coating RDX composites (NDRs)

1 g RDX was dissolved in 100 mL acetone in 60 °C water bath under stirring. 0.5 g DND was dispersed in 100 mL anhydrous ethanol while 0.05 mL Span-80 was added as surfactant. The solution was treated by ultrasonic oscillation for more than 1 h until DND was completely dispersed. The dispersion was put onto a magnetic stirring device and heated to 60 °C under 60 rpm stirring. Meanwhile, the warm RDX-acetone solution was added dropwise into the DND dispersion. After dropping, the mixed solution was kept stirring for 30 min, then quickly transferred into a vacuum distillation flask and distilled by using a rotary evaporator with a rotation speed of 45 rpm at 80 °C. After *ca.* 80% solvent was removed, the remaining thick slurry was filtrated rapidly and washed by 10 mL anhydrous ethanol and 20 mL deionized water (small amount but many times). The filter cake was dried at 40 °C for 24 h, obtaining the gray-black

powder. To determine the optimal amount of surfactant, the amounts of Span-80 were changed to 0.10 ml, 0.15 ml, 0.20 ml and 0.25 ml, respectively; while other conditions were remain unchanged. To determine the optimal coating amount of DND, the mass proportions of DND to RDX were held to 1:8 (NDR1), 1:6 (NDR2), 1:4 (NDR3) and 1:2 (NDR4) which correspond to increasing DND coating amounts of 1/9, 1/7, 1/5 and 1/3, respectively.

Apparatus and methods

Thermogravimetric analysis (TG) and differential scanning calorimetry (DSC) were applied to study the complete thermal decomposition under linear heating. Pyris-1 TGA (Perkin-Elmer, USA) was employed with an unsealed platinum pan. Less than 0.5 mg of sample was heated from 50 °C to 500 °C at the rates of 5.0, 10.0, 15.0 and 20.0 °C min⁻¹ respectively. The atmosphere was high-purity nitrogen at a flowing rate of 20.0 mL min⁻¹ under a pressure of 0.2 MPa. Pyris-1 DSC (Perkin-Elmer, USA) was used with an uncovered aluminium crucible. Less than 0.5 mg of sample was heated from 50 °C to 500 °C at the rate of 10.0 °C min⁻¹ in a dynamic nitrogen atmosphere.

Dynamic pressure measuring thermal analysis (DPTA,) is generally used to study the initial thermal decomposition at a constant low temperature in order to evaluate thermal stability.^{30, 31} Sample was weighed 1.0000±0.0010 g and loaded in an explosion-proof glass test tube. Then, the tube was sealed and evacuated to an initial pressure of less than 0.10 kPa. After being put in to the thermostat, it was held at 100 °C for 48 h.

Results and discussion

Morphology characterization

The as-prepared DND possesses a spherical shape with a average particle size of 30 nm (**Fig. 1a~b**) and a specific surface area of 237.952 m² g⁻¹ tested by multipoint BET method. The characteristic diffraction peaks of powder-XRD (**Fig. 1c**) have one strong peak (111) and two weak peaks (220) and (311), and the absence of graphite peak at $2\theta = 20\sim 30^\circ$, indicating the product was well-purified cubic DND.

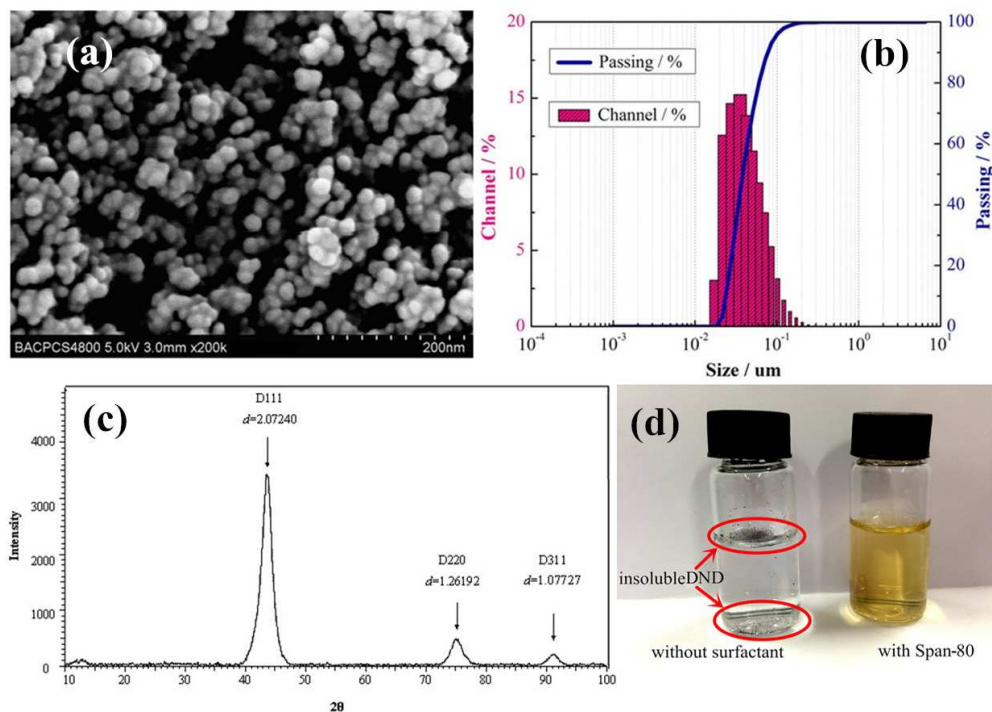


Fig. 1 Characteristics of the as-prepared DND: (a) SEM image, (b) particle size analysis, (c) powder-XRD image, and (d) digital image of DND dispersed in anhydrous ethanol. Left: without or with less than 0.15 mL Span-80, DND is suspended partly and deposited partly in the solvent; right: DND is well-dispersed with no sedimentation with 0.15~0.20 mL Span-80.

The production of the stable suspension of DND in solvent is an essential precondition for fabrication of the DND coating materials. In this study, DND avoids excessive agglomeration and results in uniform dispersion in solvent with the aid of 0.15~0.20 mL Span-80 during preparation and coating (**Fig. 1d**).

The micron scale RDX was used as the substrate material for coating (**Fig. 2a**). The DND particles were deposited and absorbed on the surface of RDX and evenly coated over RDX, and the coating thickness increased as the amount of DND increased from NDR1 to NDR4 (**Fig. 2b~e**).

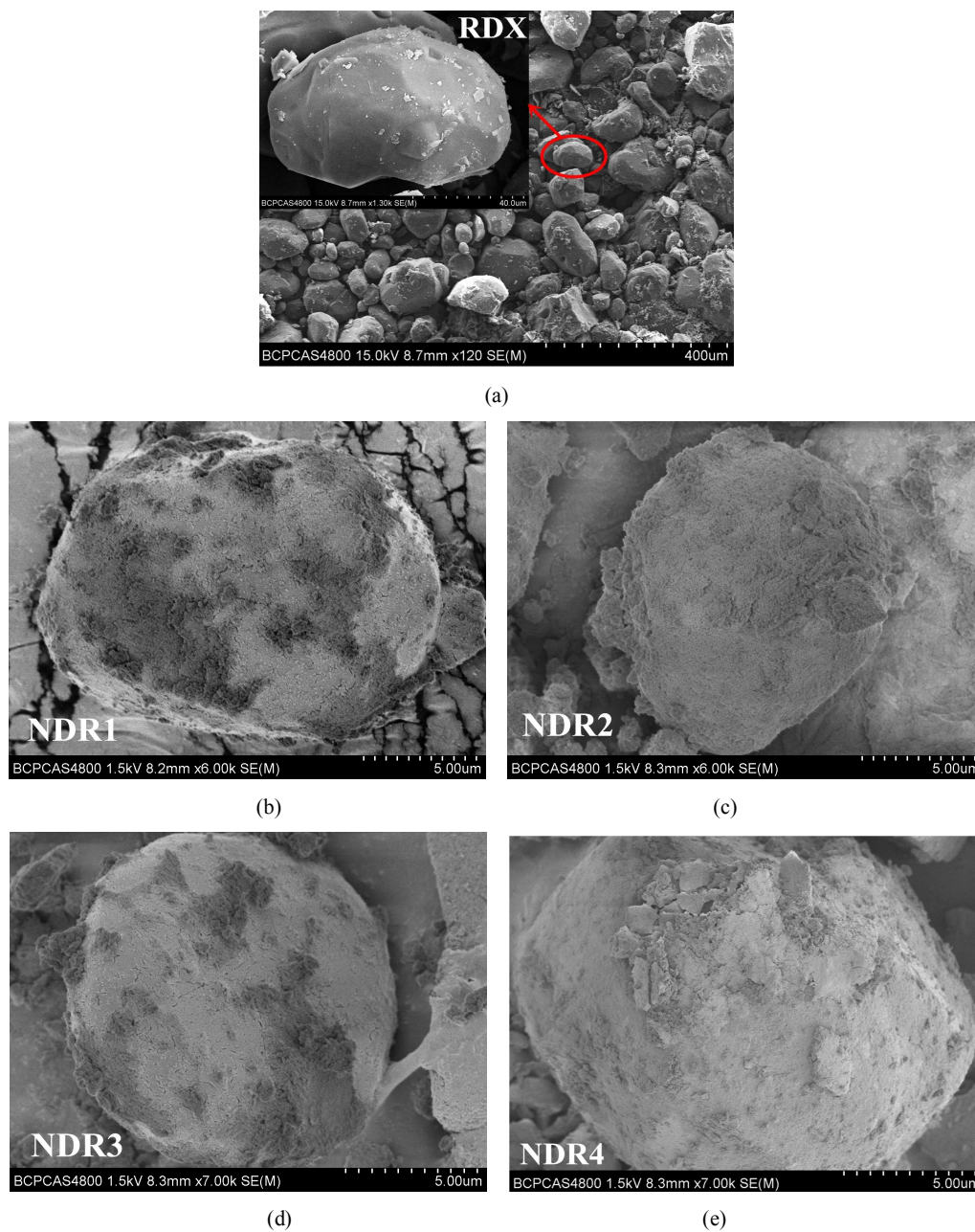


Figure 2 SEM images of RDX and NDRs

DCS analysis

The DSC curves of NDRs at the heating rate of $10.0\text{ }^{\circ}\text{C min}^{-1}$ were recorded as shown in **Fig. 3**.

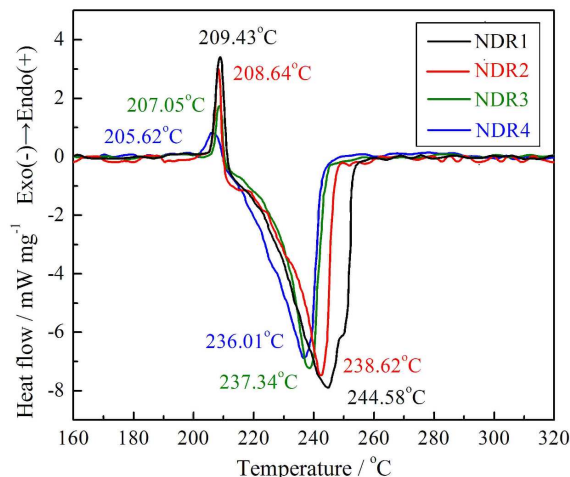


Fig. 3 DSC curves of NDRs

All the samples exhibit two acute peaks during heating; the first endothermic peak is caused by melting and the second exothermic peak by a sharp thermal decomposition. It indicates that the thermal decomposition of NDRs is a melted liquid phase reaction, just like that of pure RDX.^{32, 33} The coating DND does not change the reaction phase state. The detailed DSC data are summarized in **Table 1**.

Table 1 DSC Parameters of NDRs at heating rate of 10.0 °C min⁻¹ [a]

Samples	Endothermic peaks				Exothermic peaks			
	T_o / °C	T_p / °C	T_e / °C	ΔH_1 / J g ⁻¹	T_o / °C	T_p / °C	T_e / °C	ΔH_2 / J g ⁻¹
NDR1	203.88	209.43	210.99	68.92	217.92	244.58	259.67	-894.63
NDR2	203.54	208.64	210.04	44.25	217.42	238.62	255.35	-747.71
NDR3	202.26	207.05	209.37	23.79	215.06	237.34	252.56	-625.64
NDR4	200.63	205.62	207.86	22.92	213.37	236.01	249.27	-582.22

[a] T_o —onset temperature; T_p — peak temperature; T_e — end temperature; ΔH_1 — heat absorption; ΔH_2 — heat release.

It can be seen that the peak temperatures of melting and thermal decomposition both decrease with increasing DND coating amount from NDR1 to NDR4. The DND coating reduces the melting temperature due to the interaction of the components. Meanwhile, the coating catalyzes the decomposition of NDR because of the high reactivity of DND. As the DND coating amount increases, the proportion of RDX that is the main reaction ingredient decreases, thus the enthalpies of the endothermic and exothermic decompositions (ΔH_1 and ΔH_2) decrease from NDR1 to NDR4.

TG/DTG analysis

The thermal decomposition behaviors of all NDRs were further investigated by TG/DTG analysis under several heating rates. In order to make a quantitative comparison, the characteristic

parameters of the TG/DTG curves are summarized in **Table 2**.

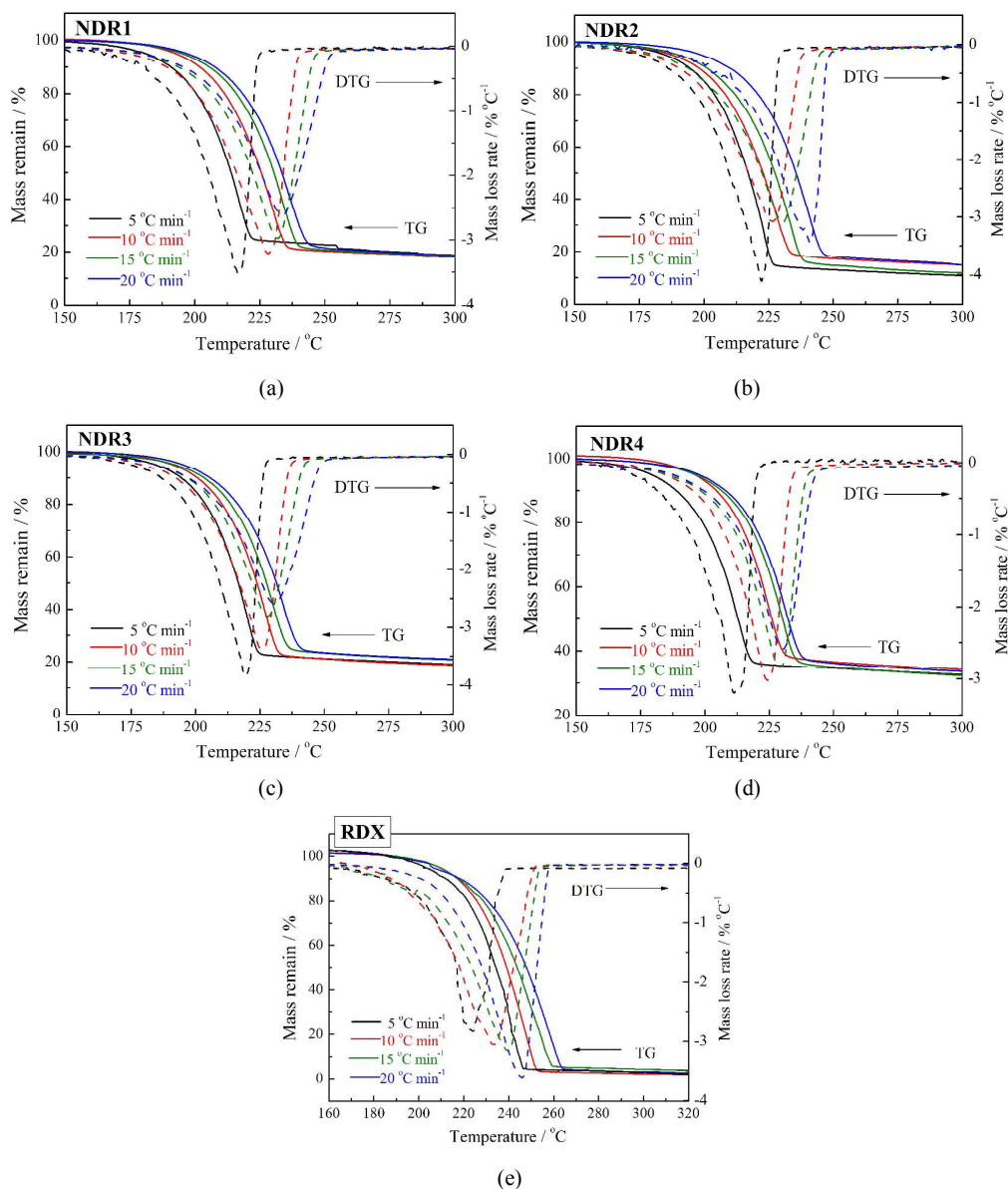


Fig. 4 TG/DTG curves of NDRs and RDX

As shown in **Fig. 4**, the TG curves of NDRs are similar to that of RDX; only a single decomposition process has been observed for all involved materials. The materials decompose completely because the mass losses are in good agreement with the contents of RDX which is the main reactant. The residues are mostly derived from the unreacted DND. With the increase of heating rate, the decomposition temperature shifts to high temperature and the maximum mass loss rate (Δm_{\max}) increases (**Table 2**). Because of the complex interaction between RDX and DND, the characteristic temperatures of thermal decomposition including the critical temperature of thermal explosion (T_b) and self accelerating decomposition temperature (T_{SADT}) are more accurate

to evaluate the thermal safety than the peak temperature or the initial decomposition temperature.^{34,35} The equations of the T_b and T_{SADT} are as follows:

$$T_{p0} = T_p - (a\beta + b\beta^2) \quad (1)$$

$$T_b = \frac{E_a - (E_a^2 - 4E_a RT_{p0})^{1/2}}{2R} \quad (2)$$

$$T_{SADT} = T_b - \frac{RT_b^2}{E_a} \quad (3)$$

Where T_p is peak temperature of DSC curve (K), T_{p0} is peak temperature when β tends to zero (K).

Table 2 Characteristic parameters from non-isothermal TG/DTG data of NDRs ^[a]

Samples	Curve characteristic parameters			Characteristic temperatures	
	$\beta / ^\circ\text{C min}^{-1}$	$T_p / ^\circ\text{C}$	$\Delta m_{\text{max}} / \% \text{ min}^{-1}$	$T_b / ^\circ\text{C}$	$T_{\text{SADT}} / ^\circ\text{C}$
NDR1	5.0	216.51	-17.81	215.14	199.78
	10.0	230.26	-32.54		
	15.0	233.85	-44.94		
	20.0	236.87	-52.48		
NDR2	5.0	223.58	-20.49	233.79	220.62
	10.0	227.20	-31.35		
	15.0	233.47	-46.74		
	20.0	239.74	-56.78		
NDR3	5.0	220.04	-19.38	223.75	213.38
	10.0	226.80	-34.22		
	15.0	229.82	-42.82		
	20.0	234.24	-52.16		
NDR4	5.0	212.78	-15.33	210.73	196.52
	10.0	224.53	-31.78		
	15.0	229.76	-39.54		
	20.0	231.17	-46.27		
RDX	5.0	218.43	-18.83	221.58	206.52
	10.0	230.62	-30.28		
	15.0	232.90	-46.05		
	20.0	239.01	-65.28		

^[a] β — heating rate; T_p — peak temperature of mass loss rate; Δm_{max} — maximum mass loss rate; T_b — critical temperature of thermal explosion; T_{SADT} — self accelerating decomposition temperature.

The T_b and T_{SADT} increase in the same order of $NDR4 < NDR1 < NDR3 < NDR2$ that conforms to a volcano-shaped curves, of which NDR2 and NDR3 have higher temperature than RDX (Fig. 5). Higher temperature indicates better thermal safety. Thus, the DND coating amount ranging from 1/7 to 1/5 provides NDR with better thermal safety than RDX, whereas too much or too little coating decreases the thermal safety but increases the reaction activity.

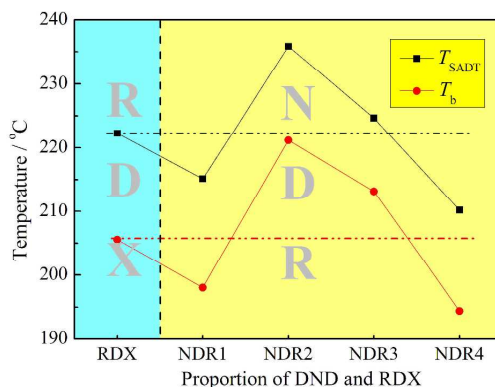


Fig. 5 Dependences of T_b and T_{SADT} on proportion of DND and RDX

The kinetic parameters of thermal decomposition of NDRs were calculated according to the Kissinger and Ozawa methods based on the shift of peak temperatures with heating rate.³⁶ The calculation results are summarized in Table 3.

Table 3 Kinetic and thermodynamic parameters of NDRs from non-isothermal TG data [a]

Samples	Kinetic parameters					Thermodynamic parameters		
	Kissinger method			Ozawa method		$\Delta H^\ddagger /$ kJ mol ⁻¹	$\Delta S^\ddagger /$ J K ⁻¹ mol ⁻¹	$\Delta G^\ddagger /$ kJ mol ⁻¹
	$E_{aK} /$ kJ mol ⁻¹	$\lg(A_K / s^{-1})$	r_K	$E_{aO} /$ kJ mol ⁻¹	r_O			
RDX	134.91	12.08	-0.9832	136.21	-0.9850	130.92	-26.03	143.41
NDR1	127.45	11.30	-0.9781	129.09	-0.9806	123.52	-40.72	142.78
NDR2	162.21	14.96	-0.9485	162.23	-0.9531	158.11	28.98	143.79
NDR3	199.92	19.10	-0.9941	198.02	-0.9945	195.88	108.35	143.15
NDR4	135.84	12.35	-0.9825	137.00	-0.9844	131.94	-20.67	141.65

[a] E_a — apparent activation energy; A — pre-exponential factor; the subscript K and O indicate the parameters were calculated by the Kissinger and Ozawa methods, respectively; ΔS^\ddagger — entropy of activation; ΔH^\ddagger — enthalpy of activation; ΔG^\ddagger — free energy of activation.

The apparent activation energies (E_a) obtained by two methods are in substantial agreement. The increasing order is ranked as $NDR1 < RDX < NDR4 < NDR2 < NDR3$. Interestingly, the changing trend of E_a also exhibits a volcano shape (see Fig. 6).

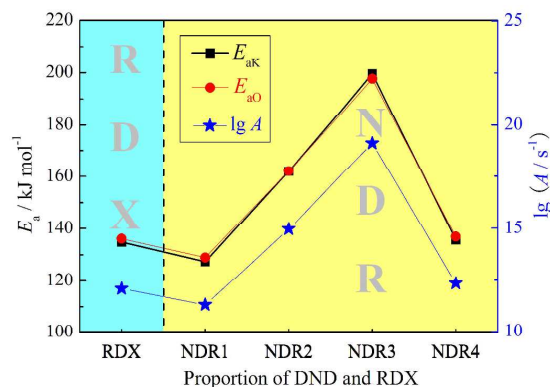


Fig. 6 Dependences of E_{aK} , E_{aO} and $\lg A$ on proportion of DND and RDX

It is well known that E_a signifies the minimum energy level that the colliding molecules must possess in order to undergo a given chemical reaction. The E_a decreases when RDX is coated by DND. Thus the DND coating could reduce the energy barrier of thermal decomposition of RDX and improve its reactivity. However, as the coating amount increases, the E_a increases from NDR1 to NDR3. Here, the activation energy theory is not reasonable enough to explain this phenomenon. In fact, the role of the pre-exponential factor A is often underestimated in kinetics analysis. The transition state theory and the collision theory hold that the pre-exponential factor A closely relates to the entropy of activation (S^\ddagger), and the large value of A indicates that the reaction molecule has high activity and collision probability.^{37, 38} Therefore, the large value of A that the nanometer- and micrometer-sized particles have is the main reason for their high reactivity.³⁹ Moreover, there is a direct proportion between E_a and A that can be interpreted as the kinetic compensation effect.^{40, 41} It indicates that the decompositions of NDRs include the same dominant and rate-determining reaction step even though there are multiple steps occurring during the whole thermal decomposition.^{42, 43} Although NDR2 and NDR3 have the larger values of E_a requiring the higher energy barriers, they also possess the larger values of A denoting their higher collision efficiencies and reaction probability. Thus, the pre-exponential factor A is the dominant factor in determining the positive correlation between the reactivity of NDR and the increasing DND coating. Unexpectedly, the sudden reversals of E_a and A occur when the coating amount is more than 1/3 for NDR4. It indicates that the effect of the DND coating amount on the thermal properties is not absolutely positive. Too much coating acts as an inert cover and reduces the reactivity of NDR4, making it more chemically stable to show the smaller values of E_a and A than other NDRs.

The thermodynamic parameters including entropy of activation ΔS^\ddagger , enthalpy of activation ΔH^\ddagger

and free energy of activation ΔG^\ddagger were determined^{44, 45} and listed in **Table 3**, and their dependences on the proportion of RDX and DND shows a similar volcano shape as the kinetic parameters as shown in **Fig. 7**.

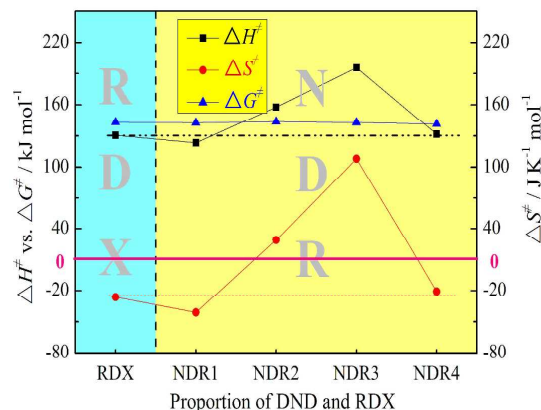


Fig. 7 Dependences of ΔS^\ddagger , ΔH^\ddagger and ΔG^\ddagger on proportion of DND and RDX

The transition state theory holds that the positive value of ΔH^\ddagger indicates that the forward activation reaction is promoted by heating, and the positive value of ΔG^\ddagger indicates the reaction is a non-spontaneous process.⁴⁶⁻⁴⁸ On the one hand, the decompositions of NDRs are both kinetically and thermodynamically unfavorable since their activated processes in the pathway are endothermic ($\Delta H^\ddagger > 0$ and $\Delta G^\ddagger > 0$). On the other hand, the smaller ΔH^\ddagger signifies the lower heat required to start an reaction, making it less endothermic. The ΔH^\ddagger herein ranks in an increasing order of NDR1 < RDX < NDR4 < NDR2 < NDR3. Therefore, the thermal decomposition of NDR1 with the coating amount reaching 1/9 becomes more thermodynamically favorable than that of RDX. ΔS^\ddagger signifies the difference of freedom degree between activated transition state and reactant; $\Delta S^\ddagger > 0$ means that the transition state possesses more activated reaction sites and greater confusion degree than the reactant. The ΔS^\ddagger is ordered as NDR1 < RDX < NDR4 < 0 < NDR2 < NDR3. NDR2 and NDR3 have positive values of ΔS^\ddagger , implying that their transition states in the thermal decomposition are probably the dissociated compounds rather than the combined complexes. Thus, the DND coating and its coating amount could affect the reaction mechanisms. However, since the contribution of ΔS^\ddagger to ΔG^\ddagger shows no significant difference from that of ΔH^\ddagger to ΔG^\ddagger , and according to the equation $\Delta G^\ddagger = \Delta H^\ddagger - T\Delta S^\ddagger$, the effect of the coating amount on ΔG^\ddagger is negligible. On the whole, NDR1 is the most preferential both in thermodynamics and kinetics of thermal decomposition because it has the smallest values of ΔH^\ddagger and ΔS^\ddagger . Therefore, the smaller DND coating amount leads NDR to be more thermodynamically and kinetically favorable.

DPTA analysis

DPTA was used to study the initial thermal decomposition for NDRs, which differs from the complete decomposition analyses of DSC and TG. DPTA records the time dependence of the gas pressure evolved from thermal decomposition and normalizes the pressure under standard conditions of 1.0 g sample mass, 25 mL volume and 273.15 K temperature as shown in **Fig. 8**.

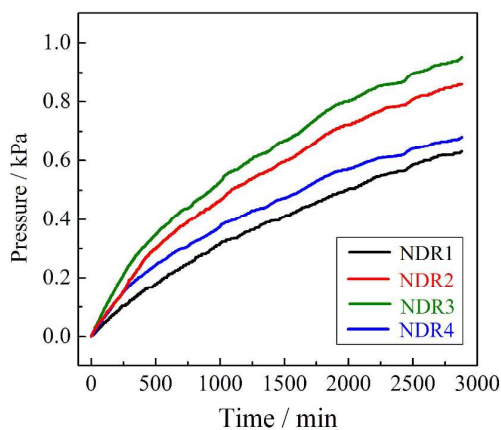


Fig. 8 Time dependences of evolved gas pressures of NDRs at 100 °C recorded by DPTA

The DPTA curves for all involved materials basically obey a parabolic trend with heating time. At the beginning stage within 500 min, all the pressures increase rapidly but the pressure growth rates conform to an increasing order of $\text{NDR1} < \text{NDR4} < \text{NDR2} < \text{NDR3}$. Within the remaining 2380 min, the pressure growth rates slow gradually in different degrees. It shows that the decomposition accompanied by gas emission proceeds slowly and smoothly in a long duration. On the whole, the increasing order of the total gas emission is $\text{NDR1} < \text{NDR4} < \text{NDR2} < \text{NDR3}$. The gas emission represented by the standard-state volume (V) is used to characterize the thermal stability of energetic materials; less gas signifies greater stability. Good thermal stability requires $V < 2.00 \text{ mL g}^{-1}$ at 100 °C.^{49, 50} The gas emission amounts of NDRs are listed in **Table 4**.

Table 4 Gas emission and reaction rate constant of NDRs from DPTA data ^[a]

Samples	Gas emission		Kinetic parameters		
	$p / \text{kPa g}^{-1}$	$V / \text{mL g}^{-1}$	$k / 10^{-7} \text{ s}^{-1}$	$b^{[a]}$	r
NDR1	0.6298±0.0315	0.1554±0.0078	4.10	-0.01019	0.9977
NDR2	0.8572±0.0408	0.2115±0.0102	4.24	-0.02830	0.9986
NDR3	0.9526±0.0453	0.2333±0.0115	4.28	-0.01503	0.9987
NDR4	0.6806±0.0340	0.1680±0.0083	4.19	-0.01078	0.9982

^[a] b denotes the intercept of the line of solid phase reaction kinetic equation $G(a) = ka + b$, and r is linear correlation coefficient. According to the smallest b and largest r , the most probable k was selected by the model

fitting method.

All samples have excellent thermal stability within the given temperature range. The increasing order of the thermal stability follows $\text{NDR3} < \text{NDR2} < \text{NDR4} < \text{NDR1}$. The previous report on the gas emission of RDX is about 0.10 mL g^{-1} . Thus, the coating DND catalyzes the decomposition of the main reactant RDX in NDR. It is known to all that DND possesses many advantages of small size effect, huge surface effect and high thermal conductivity. As the coating amount increases, the interaction between DND and RDX becomes more violent and the heat conduction among particles becomes faster, thus catalyzing the decomposition of RDX and resulting in greater gas production within given time. However, when the coating amount reaches $1/3$ corresponding to NDR4, too much DND covers the surface of RDX and hinders in some degree the decomposition of RDX and the diffusion of gaseous products, the gas emission therefore decreases conversely. Nevertheless, the catalysis of DND is still greater than their covering effect on RDX so NDR decomposes and releases more gas than RDX. The catalytic mechanism could be due to the interaction between DND and the gaseous products in the case of partial equilibrium; however, the definite mechanism needs further study. It can be concluded that the appropriate coating amount has great effect on the thermal properties of composite. The appropriate DND coating not only maintains the good stability and compatibility of NDR but also moderately improves its initial thermal decomposition behavior.

The reaction rate constants was fitted by the solid phase reaction kinetic equation³⁶ and listed in **Table 4**. The reaction rate constants arranged in an increasing order is $\text{NDR1} < \text{NDR4} < \text{NDR2} < \text{NDR3}$. The k increases as the DND coating amount increases; however, it decreases conversely when the coating amount reaches more than $1/3$. The appropriate amount of DND coating accelerates the thermal decomposition largely due to the interaction between DND and RDX or the secondary reaction between DND and the decomposition products. On the contrary, excessive coating, like a layer of protective shell, hinders the further decomposition and the gas emission.

Isoconversional kinetics analysis

Through the kinetic analyses of TG and DPTA, it have been concluded that the thermal decompositions of NDRs include multiple steps and the occurrence of interaction between components catalyzes the decomposition. To further prove this result, the activation energy dependence on the extent of conversion (E_a vs. α) evaluated by the isoconversional kinetics was

applied. Because the isoconversional principle describes that a single step process has an invariable E_a vs. α ; conversely, a variation of E_a vs. α indicates the occurrence of a multi-step process.⁵¹⁻⁵³ The α - T curves of NDRs are plotted and shown in Fig. 9. It can be seen that all of the decomposition curves basically obey a sigmoidal trend.

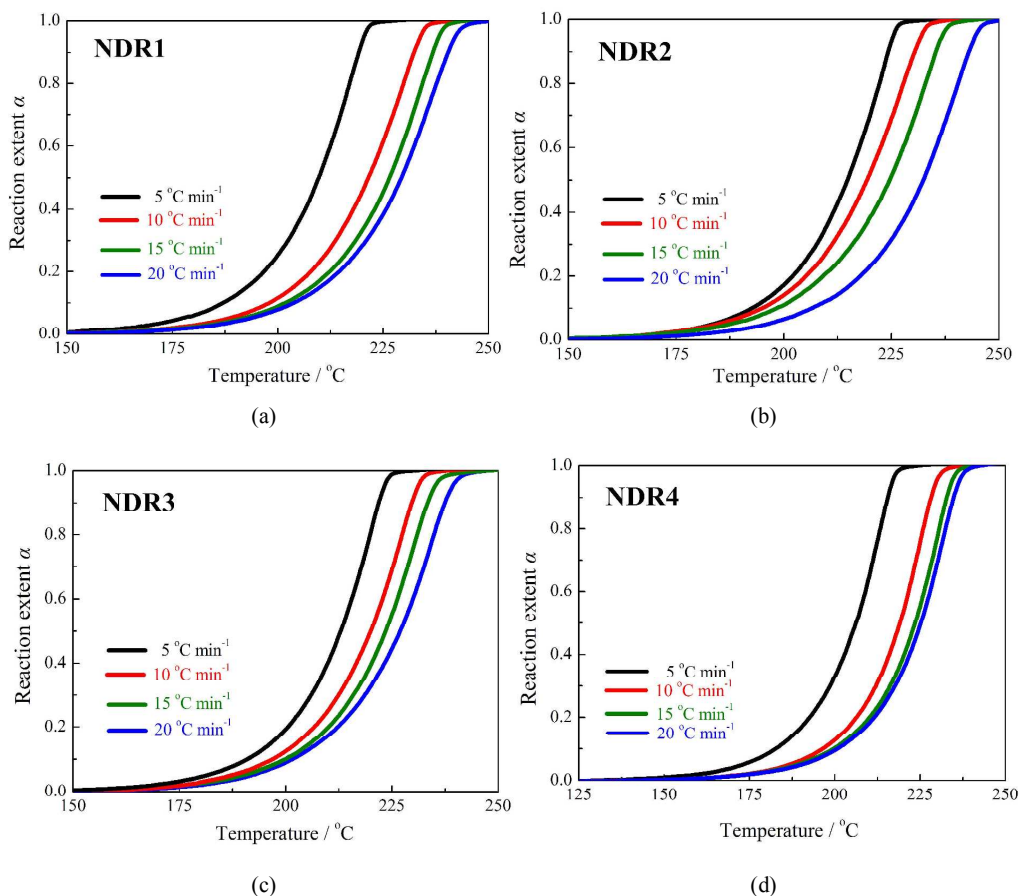


Fig. 9 α - T curves of NDRs under different heating rates

According to International Confederation for Thermal Analysis and Calorimetry (ICTAC) Kinetics Committee recommendation⁵⁴, a more accurate equation called the Kissinger-Akahira-Sunose (KAS) equation⁵⁵ was used herein to calculate the isoconversional kinetics. The corresponding results are summarized in Table 5.

Table 5 Isoconversional kinetics of NDRs by KAS method

α	NDR1		NDR2		NDR3		NDR4	
	E_a / kJ mol ⁻¹	r						
0.1	133.99±17.	-0.98	156.71±55.	-0.89	227.73±14.	-0.99	115.25±24.	-0.95
	63	31	87	29	17	62	78	68
0.2	134.95±15.	-0.98	148.60±49.	-0.90	218.48±7.1	-0.99	118.05±23.	-0.96

	93	64	39	50	9	89	39	29
0.3	133.41±13.	-0.98	147.71±40.	-0.93	210.61±3.7	-0.99	122.41±22.	-0.96
	84	94	46	25	3	97	17	87
0.4	132.21±12.	-0.99	146.90±35.	-0.94	201.14±3.1	-0.99	124.14±20.	-0.97
	34	14	34	67	4	98	39	41
0.5	130.67±11.	-0.99	147.13±34.	-0.94	194.53±5.4	-0.99	126.99±19.	-0.97
	87	18	27	98	2	92	42	74
0.6	130.37±12.	-0.99	147.66±32.	-0.95	190.85±6.4	-0.99	130.38±20.	-0.97
	72	06	98	36	7	89	15	69
0.7	130.43±13.	-0.98	149.19±31.	-0.95	188.62±8.8	-0.99	130.66±19.	-0.97
	34	97	51	82	3	78	42	86
0.8	128.11±13.	-0.98	150.31±29.	-0.96	186.66±8.1	-0.99	131.70±18.	-0.98
	61	89	74	30	7	81	06	17
0.9	127.01±13.	-0.98	147.39±26.	-0.96	182.93±6.5	-0.99	132.52±17.	-0.98
	71	86	92	82	8	87	41	32
Mean	131.24		149.07		200.18		125.79	
SD	2.50		2.89		14.67		5.88	
Mean								
($\alpha =$	128.98		148.64		187.26		131.31	
0.6~0.9)								
SD								
($\alpha =$	1.47		1.19		2.91		0.85	
0.6~0.9)								

The E_a vs. α ($\alpha = 0.1, 0.2, 0.3, \dots, 0.9$) dependences of NDRs were shown in **Fig. 10** for a clear comparison.

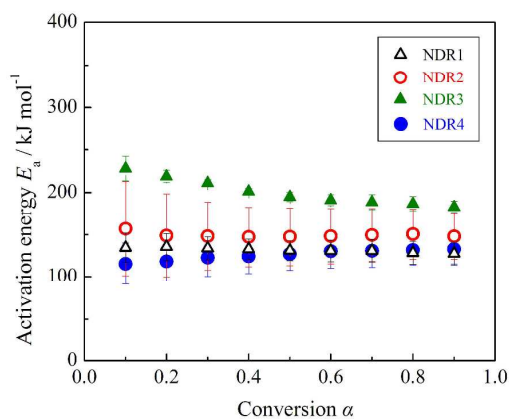


Fig. 10 Dependences of E_a vs. α by KAS method

There is an evidence of a multi-step reaction mechanism for the thermal decomposition of NDRs, because the isoconversional activation energies (E_a) vary with conversion extent (α), especially at the initial decomposition stage where $\alpha = 0.1\sim 0.5$. The DND could greatly affect the

activation energy of the initial thermal decomposition, making it more dependent on the conversion extent. It proves that DND plays an important role in catalyzing the thermal decomposition of NDRs. However, at the stage of $\alpha = 0.6\sim 0.9$, the E_a s of all NDRs are almost independent on α . It indicates that the secondary reaction and the catalytic reaction could diminish or disappear, that is, the effect of the DND coating decreases gradually as the decomposition proceeds. Therefore, the average activation energies obtained by KAS method at $\alpha = 0.6\sim 0.9$ might be more physically meaningful, because the significantly changing stage of the reaction mechanism was alleviated. The average activation energies without using the data from $\alpha = 0.1\sim 0.5$ are arranged in an increasing order of $\text{NDR1} < \text{NDR4} < \text{NDR2} < \text{NDR3}$. This order is consistent with that obtained by traditional Kissinger method. In fact, it is extremely difficult to obtain intrinsic kinetic parameters of a reaction that are not affected by kinetic contributions from other steps and diffusion. Generally, the effective kinetic parameters are the complex functions of the intrinsic kinetic parameters of the individual steps.⁵⁴ Therefore, this work is concerned with the analysis of the apparent kinetic parameters which tend to vary with conversion extent and temperature, but they can be employed to make reliable kinetic predictions, to get information about complex mechanisms.

Conclusions

The DND with the size of 30nm was prepared and successfully coated over the micron-sized RDX in different coating amounts. The morphologies of NDRs were characterized by SEM, and their thermal decomposition and kinetics were studied by DSC, TG and DPTA techniques. The effect of DND coating amount on the thermal properties was investigated. The following conclusions are made:

- 1) The thermal safety of NDRs characterized by T_b and T_{SADT} increases in an order of $\text{NDR4} < \text{NDR1} < \text{RDX} < \text{NDR3} < \text{NDR2}$. The DND coating amount ranging from 1/7 to 1/5 corresponding to NDR2 and NDR3 provides NDRs with better thermal safety than pure RDX.
- 2) The kinetic parameters E_a and A show the same increasing order of $\text{NDR1} < \text{NDR4} < \text{NDR2} < \text{NDR3}$. The effects of E_a and A on the reactivity should be concerned together. The large E_a indicates the high energy barrier required but the large A indicates the high collision efficiency and reaction probability. Therefore, the reactivity of NDR increases with increasing DND

coating amount, but the coating amount more than 1/3 hinders the decomposition and reduces the reactivity.

- 3) The thermodynamic parameters ΔG^\ddagger appears nearly independent of the coating amount, while ΔH^\ddagger and ΔS^\ddagger are both ordered as $\text{NDR1} < \text{RDX} < \text{NDR4} < \text{NDR2} < \text{NDR3}$. It indicates that the DND coating amount of 1/9 corresponding to NDR1 makes the thermal decomposition of RDX more thermodynamically and kinetically favorable.
- 4) The gas emission and the reaction rate constants obtained by DPTA analysis exhibit the same order of $\text{NDR1} < \text{NDR4} < \text{NDR2} < \text{NDR3}$. The coating DND could catalyze the decomposition of RDX, because DND possesses the small size effect, huge surface effect and high thermal conductivity which promotes heat conduction among particles and enhances the interaction between DND and RDX. However, excessive coating acting as inert layer blocks the gas emission. Therefore, only the appropriate DND coating amount efficiently improves the thermal properties of NDRs.
- 5) The isoconversional E_a s of all NDRs calculated by KAS method vary with α when $\alpha = 0.1\sim 0.5$, indicating that the thermal decomposition of NDRs includes multiple steps. However, these E_a are almost constant with α when $\alpha = 0.6\sim 0.9$. It suggests that the catalytic effect of DND could decrease gradually as the decomposition proceeds.

Acknowledgements

This work was financially supported by the Science and Technology Fund on Applied Physical Chemistry Laboratory (Nos. 9140C3703051105 and 9140C370303120C37142), and the Key Support Foundation of State Key Laboratory of Explosion Science and Technology (Nos. QNKT12-02 and YBKT 10-05).

References

- 1 R. J. Narayan, R. D. Boehm and A. V. Sumant, *Mater. Today*, 2011, **14**, 154-163.
- 2 A. Krueger, *J. Mater. Chem.*, 2011, **21**, 12571-12578.
- 3 V. N. Mochalin, O. Shenderova, D. Ho and Y. Gogotsi, *Nat. Nanotechnol.*, 2012, **7**, 11-23.
- 4 A. Krueger, *Adv. Mater.*, 2008, **20**, 2445-2449.
- 5 R. K. Ahmad, A. C. Parada, S. Hudziak, A. Chaudhary and R. B. Jackman, *Appl. Phys. Lett.*, 2010, **97**, 093103.
- 6 A. Thalhammer, R. J. Edgington, L. A. Cingolani, R. Schoepfer and R. B. Jackman, *Biomaterials*, 2010, **31**, 2097-2104.

- 7 L. Cunci and C. R. Cabrera, *Electrochem. Solid-ST.*, 2011, **14**, K17-K19.
- 8 K. Hristova, E. Pecheva, L. Pramatarova and G. Altankov, *J. Mater. Sci.*, 2011, **22**, 1891-1900.
- 9 J. Kaleicheva, Z. K. Karaguiozova, E. Lyubchenko, M. Kandeve, V. Mishev and S. Stavrev, *J. Chem. Chem. Eng.*, 2012, **6**, 599-603.
- 10 L. La-Torre-Riveros, R. Guzman-Blas, A. n. E. Méndez-Torres, M. Prelas, D. A. Tryk and C. R. Cabrera, *ACS appl. Mater. Inter.*, 2012, **4**, 1134-1147.
- 11 Y. Li, C. Zhang, H. Ma, L. Yang, L. Zhang, Y. Tang, X. Li, L. He, R. Feng and Q. Yang, *Mater. Chem. Phys.*, 2012, **134**, 145-152.
- 12 A. Dhakshinamoorthy, S. Navalon, D. Sempere, M. Alvaro and H. Garcia, *Chem. Commun.*, 2013, **49**, 2359-2361.
- 13 A. Ermakova, G. Pramanik, J. M. Cai, G. Algara-Siller, U. Kaiser, T. Weil, Y. K. Tzeng, H. C. Chang, L. P. McGuinness and M. B. Plenio, *Nano lett.*, 2013, **13**, 3305-3309.
- 14 R. Velázquez, V. F. Neto, K. Uppireddi, B. R. Weiner and G. Morell, *Coatings*, 2013, **3**, 243-252.
- 15 T. Khamova, O. Shilova, G. Kopitsa, L. Almásy and L. Rosta, *Phys. Solid State*, 2014, **56**, 105-113.
- 16 M. Abdoli and A. Sabour Rouhaghdam, *Diam. Relat. Mater.*, 2013, **31**, 30-37.
- 17 D. M. Badgular, M. B. Talawar, S. N. Asthana and P. P. Mahulikar, *J. Hazard. Mater.*, 2008, **151**, 289-305.
- 18 M. Fathollahi, B. Mohammadi and J. Mohammadi, *Fuel*, 2013, **104**, 95-100.
- 19 V. Strunin and L. Nikolaeva, *Combust. Explor. Shock.*, 2013, **49**, 53-63.
- 20 M. B. Talawar, R. Sivabalan, T. Mukundan, H. Muthurajan, A. K. Sikder, B. R. Gandhe and A. S. Rao, *J. Hazard. Mater.*, 2009, **161**, 589-607.
- 21 T. M. Klapotke and G. Steinhauser, *Angew. Chem. Int. Ed.*, 2008, **47**, 3330-3347.
- 22 Y. L. Zhu, H. Huang, H. Ren and Q. J. Jiao, *J. Energ. Mater.*, 2013, **31**, 178-191.
- 23 X. QI, X. ZHANG, Q. YAN, Z. SONG, P. LIU and J. LI, *Chem. Propell. Polym. Mater.*, 2012, **1**, 016.
- 24 X. G. Wu, Q. L. Yan, X. Guo, X. F. Qi, X. J. Li and K. Q. Wang, *Acta Astronaut.*, 2011, **68**, 1098-1112.
- 25 J. M. Gao, L. Wang, H. J. Yu, A. G. Xiao and W. B. Ding, *Propell. Explos., Pyrot.*, 2011, **36**, 404-409.
- 26 J. Luman, B. Wehrman, K. Kuo, R. Yetter, N. Masoud, T. Manning, L. Harris and H. Bruck, *Proceedings of the Combustion Institute*, 2007, **31**, 2089-2096.
- 27 V. Y. Dolmatov, *Russ. Chem. Rev.*, 2001, **70**, 607.
- 28 V. Y. Dolmatov, *Russ. Chem. Rev.*, 2007, **76**, 339.
- 29 V. Danilenko, *Phys. Solid State*, 2004, **46**, 595-599.
- 30 R. Liu, Z. Zhou, Y. Yin, L. Yang and T. Zhang, *Thermochim. Acta*, 2012, **537**, 13-19.
- 31 R. Liu, T. Zhang, L. Yang and Z. Zhou, *Cent. Eur. J. Chem.*, 2014, **12**, 672-677.
- 32 G. Hussain and G. J. Rees, *Fuel*, 1995, **74**, 273-277.
- 33 J. S. Lee, C. K. Hsu and C. L. Chang, *Thermochim. Acta*, 2002, **392**, 173-176.
- 34 J. H. Yi, F. Q. Zhao, B. Z. Wang, T. An, Y. Wang and H. X. Gao, *J. Therm. Anal. Calorim.*, 2014, **115**, 1227-1234.
- 35 B. Yan, H. X. Ma, N. N. Zhao, T. Mai, J. R. Song, F. Q. Zhao and R. Z. Hu, *J. Therm.*

- Anal. Calorim.*, 2012, **110**, 1253-1257.
- 36 R. Z. Hu, S. L. Gao, F. Q. Zhao, Q. Z. Shi, T. L. Zhang and J. J. Zhang, *Thermal Analysis Kinetics* second ed, Science Press, Beijing, 2008.
- 37 P. Pechukas and F. J. McLafferty, *J. Chem. Phys.*, 1973, **58**, 1622-1625.
- 38 K. Morokuma, B. C. Eu and M. Karplus, *J. Chem. Phys.*, 1969, **51**, 5193-5203.
- 39 R. Liu, W. Yu, T. Zhang, L. Yang and Z. Zhou, *Phys. Chem. Chem. Phys.*, 2013, **15**, 7889-7895.
- 40 P. J. Barrie, *Phys. Chem. Chem. Phys.*, 2012, **14**, 318-326.
- 41 P. J. Barrie, *Phys. Chem. Chem. Phys.*, 2012, **14**, 327-336.
- 42 A. K. Galwey and M. Mortimer, *Inter. J. Chem. Kinet.*, 2006, **38**, 464-473.
- 43 J. G. R. Poco, H. Furlan and R. Giudici, *J. Phys. Chem. B*, 2002, **106**, 4873-4877.
- 44 R. Liu, L. Yang, Z. Zhou and T. Zhang, *J. Therm. Anal. Calorim.*, 2014, **115**, 1939-1948.
- 45 R. Liu, T. Zhang, L. Yang and Z. Zhou, *Thermochim. Acta*, 2014, **583**, 78-85.
- 46 D. G. Truhlar, B. C. Garrett and S. J. Klippenstein, *J. Phys. Chem.*, 1996, **100**, 12771-12800.
- 47 D. G. Truhlar, W. L. Hase and J. T. Hynes, *J. Phys. Chem.*, 1983, **87**, 2664-2682.
- 48 R. Gounder and E. Iglesia, *Accounts Chem. Res.*, 2011, **45**, 229-238.
- 49 GJB 772A-97. Method 501.2: Vacuum stability test - Method of pressure transducer. Commission of Science, Technology and Industry for National Defense. Beijing; 1997. pp. 156-158.
- 50 GJB 5891.12 - 2006. Test method of loading material for initiating explosive device - Part 12: Vacuum stability test - Method of pressure transducer. Commission of Science, Technology and Industry for National Defense. Beijing; 2006. pp. 67-70.
- 51 M. Venkatesh, P. Ravi and S. P. Tewari, *J. Phys. Chem. A*, 2013, **117**, 10162-10169.
- 52 W. Wu, J. Cai and R. Liu, *Ind. Eng. Chem. Res.*, 2013, **52**, 14376-14383.
- 53 S. Vyazovkin and N. Sbirrazzuoli, *Macromol. Rapid Comm.*, 2006, **27**, 1515-1532.
- 54 S. Vyazovkin, A. K. Burnham, J. M. Criado, L. A. Perez-Maqueda, C. Popescu and N. Sbirrazzuoli, *Thermochim. Acta*, 2011, **520**, 1-19.
- 55 M. J. Starink, *Thermochim. Acta*, 2003, **404**, 163-176.